Highly efficient application of activated carbon as catalyst for wet peroxide oxidation

C.M. Domínguez [a],[*], P. Ocón [b], A. Quintanilla [a], J.A. Casas [a], J.J. Rodriguez [a]

[a] Área de Ingeniería Química, Universidad Autónoma de Madrid, Campus de Cantoblanco, 28049 Madrid, Spain
[b] Departamento de Química Física Aplicada, Facultad de Ciencias Químicas, Universidad Autónoma de Madrid, Campus de Cantoblanco, 28049 Madrid, Spain

ABSTRACT

This paper addresses the improved performance of activated carbons in catalytic wet peroxide oxidation (CWPO) of phenol as target compound. Initial cyclic voltammetry experiments show that hydrogen peroxide and phenol compete for the same active sites on the carbon surface. Then, a significant coverage of the carbon surface by phenol molecules is the approach attempted to increase the efficiency of hydrogen peroxide and the performance of the oxidation process.

In this work, two commercial activated carbons, with different physical and electrochemical properties have been tested. The results demonstrate that working at high phenol concentration (5 g/L) and phenol/carbon mass ratio (2), unprecedented hydrogen peroxide efficiencies of around 100% are achieved, allowing high oxidation and mineralization degrees, *i.e.* 97% phenol and 70% TOC conversions at 80 °C with the stoichiometric dose of hydrogen peroxide required for complete mineralization of phenol. The oxidation route of phenol in the presence of activated carbon is also studied and a reaction pathway proposed. Resorcinol was a new by-product detected whose formation occurs upon reaction on the carbon surface. Condensation by-products, typically formed in Fenton oxidation of phenol, were not found in the effluents but adsorbed on the carbon surface causing a progressive deactivation upon use. The activity can be easily recovered by oxidative thermal regeneration (350 °C, 24 h).

© 2013 Elsevier B.V. All rights reserved.

1. Introduction

Catalytic wet peroxide oxidation (CWPO) relies on the oxidation of organic pollutant in water under relatively mild operating conditions ($T = 25$–100 °C, $P = 0.1$–0.5 MPa) using hydrogen peroxide as oxidant.

Activated carbons (ACs) have been used as catalysts in CWPO [1–11] since they exhibit donor–acceptor surface properties allowing hydrogen peroxide decomposition into radical species through an electron transfer reaction similar to the Fenton mechanism [12,13]. In this way, AC and AC$^+$ act as reduced and oxidized catalyst states leading to the formation of $^\bullet$OH and $^\bullet$OOH, respectively [4,5,8,10,14,15]. As studied in a previous work [16], the electrochemical capacity of a carbon material dictates the carbon activity in this reaction. Cyclic voltammetry analysis combined with kinetic studies have shown that the apparent first-order rate constant for hydrogen peroxide decomposition is linearly dependent on the exchange current, and that the limiting step in this reaction is the

regeneration of the active sites by the reduction of the carbon surface.

In spite of the widely demonstrated ability of activated carbons for hydrogen peroxide decomposition, the removal of organic pollutants in CWPO with bare ACs proceeds mostly through adsorption [1,2,11,13]. Low activities for removal of phenolic compounds [2,8,9,11] and moderate for dyes [3–5,7] have been usually observed even at hydrogen peroxide doses significantly higher than the stoichiometric ones for the complete mineralization of phenol. The efficient consumption of hydrogen peroxide is of main concern in CWPO with activated carbons. AC promotes parasitic reactions consuming $^\bullet$OH and $^\bullet$OOH radicals to produce oxygen, a non-effective specie under the temperature range commonly used in wet peroxide oxidation. That represents a serious drawback for the potential application of AC in CWPO. For this reason, transition metals, in particular Fe, and metal oxides have been incorporated onto the carbon surface. The high surface area of activated carbons provides multiple anchoring sites for the metal and a high capacity for the adsorption of organic molecules. However, metal leaching has been commonly observed.

A different approach to improve the performance of ACs has been attempted through chemical modification of the carbon surface addressed to introduce acid or basic oxygen groups

* Corresponding author. Tel.: +34 914975602; fax: +34 914973516.
E-mail addresses: carmenmaria.dominguez@uam.es,
cm.domingueztorre@gmail.com (C.M. Domínguez).

[3–5,7,9]. According to some results, acid groups decrease the activity of the virgin AC for hydrogen peroxide decomposition [5–7,9,15,17], while the incorporation of basic groups does the opposite [4,11,15,17]. In both cases, oxidation is enhanced but obviously due to different effects. The acid groups with electron withdrawal capacity substrate electrons from the basal planes of the carbon surface thus restricting their availability to hydrogen peroxide molecules. Therefore, radical species from hydrogen peroxide are formed more gradually and the extension of the parasitic reactions decreases while increasing the breakdown of organic species [9]. On the other hand, basic groups (pyrones, chromenes, ethers and carbonyls) enhance the decomposition of hydrogen peroxide into radicals species.

Herein, we offer a novel approach to enhance the selectivity of AC toward phenol oxidation and mineralization in detriment of the scavenging reactions, with the aim of maximizing the efficiency of hydrogen peroxide consumption. This approach consists of carrying out the CWPO at relatively high phenol concentration (5 g/L), substantially above the most commonly used and also, high phenol/carbon mass ratio. Then, a significant coverage of the carbon surface by the organic molecules should decrease the rate of radical formation from hydrogen peroxide decomposition and makes phenol more easily available to the oxidizing radicals. Both aspects reduce the occurrence of parasitic scavenging reactions on the carbon surface.

Two commercial activated carbons with different physical and electrochemical properties have been tested in CWPO using phenol as target compound. Their activity has been evaluated in relation with hydrogen peroxide decomposition and phenol oxidation and mineralization. Also, the phenol oxidation pathway in the presence of activated carbon has been investigated. Regeneration of the activated carbon after its use has been studied as well.

2. Experimental

2.1. Reagents

Aqueous phenol solutions were prepared with phenol (5 g/L) (Sigma–Aldrich) at pH 3.5 using HCl 1 M (Panreac). Hydrogen peroxide solution (30% w/w) was purchased from Sigma–Aldrich. Working standard solutions of phenol (Sigma–Aldrich), hydroquinone (Sigma–Aldrich), resorcinol (Sigma–Aldrich), catechol (Sigma–Aldrich), *p*-benzoquinone (Sigma–Aldrich), acetic acid (Sigma–Aldrich), formic acid (Sigma–Aldrich), malonic acid (Sigma–Aldrich), maleic acid (Sigma–Aldrich) and oxalic acid (Panreac) were prepared for equipment calibration. Other reagents used in the analysis were H_2SO_4 (Panreac), C_2H_3N (Riedel-deHaën), Na_2CO_3 (Panreac), $NaHCO_3$ (Merck), $Na_2S_2O_8$ (Panreac), HPO_4 (Fisher), $C_6H_4COOHCOOK$ (Aldrich), $TiOSO_4$ (Riedel-deHaën), $C_{16}H_{18}N_3ClN_3S$ (Panreac) and CH_3OH (Sigma–Aldrich). These reagents are of analytical grade and were used without further purification. All the solutions were prepared with milli-Q water.

2.2. Activated carbons

Commercial activated carbons were supplied by Merck (AC-M, ref.: 102514, granular) and Panreac (AC-P, ref.: 121237, $d_p < 100 \mu m$). Before use they were sieved to yield a particle size ranged from 80 to 100 μm. Also, the samples of activated carbons were pre-washed with a phenol solution by contacting 0.125 g of AC with 50 mL of the 5 g/L phenol solution at 80 °C during 24 h under vigorous stirring. The resulting samples were identified as w-AC-P and w-AC-M.

2.3. Characterization of the activated carbons

Different techniques were used for the characterization of the ACs used as catalysts. X-ray diffraction (XRD) was performed in a Siemens Model D5000 X-ray diffractometer, using Cu Kα (8.04 keV) radiation, and a step of 0.02°/s for $2\theta = 5°–100°$. XRD data were analyzed with PDF 2000 (JCPDS-ICDD) software.

Thermogravimetric analysis (TGA) was carried out in a Mettler-Toledo TGA/SDTA851^e thermobalance. The sample powders were heated in air from 50–900 °C at heating rate of 10 °C/min. The textural properties of fresh and pre-washed carbons were characterized from the 77 K N_2 adsorption/desorption isotherms using a Micromeritics Tristar apparatus, outgassing the samples overnight at 150 °C to a residual pressure of $<10^{-3}$ Torr. The external or non-microporous surface area (A_{ext}) and the micropore volumes (V_m) were calculated by the *t*-method. Elemental analysis was performed in a LECO Model CHNS-932 apparatus. Total reflection X-ray fluorescence (TXRF) (Extra-II Rich & Seifert spectrometer) was used for elements identification and iron content in the carbon ashes. The surface oxygen groups (SOGs) were quantified by temperature-programmed desorption (TPD). The analysis was carried out as follows: a sample of 100 mg of carbon was placed in a quartz tube and heated at 10 °C/min from room temperature up to 900 °C. N_2 was used as carrier gas at 1000 N mL/min. The evolving CO_2 and CO were analyzed in a SIEMENS (mod. Utramat 22) gas analyzer. Deconvolutions of the TPD spectra were adjusted to multiple Gaussian function by Peakfit 4.12 software.

Cyclic voltammetry measurements were carried out at room temperature and ambient pressure in a conventional three-electrode electrochemical cell, using a computerized potentiostat (Autolab PGSTAT 302, Eco Chemie) controlled by GPES software. A glassy carbon rotating disk electrode was used as substrate for the carbon samples, a gold electrode as the counter electrode, a saturated Ag/AgCl, KCl electrode as the reference and HCl solution (pH 3.5) as electrolyte. The carbon electrode was prepared by dispersing 6 mg of the activated carbon (as-received or pre-washed with a phenol solution) in Milli-Q water (730 μL) with ultrasonic agitation (Hyelscher, UP50H) and dropped on the glassy carbon electrode (20 μL) to obtain a uniform catalyst film. The prepared electrodes were subjected to cyclic voltammetry measurements (10 mV/s) under nitrogen atmosphere in the absence (background) and the presence of hydrogen peroxide (25 g/L) within the potential range from −0.6 to 1 V. From these experiments, the coulombic charge (CC) and the exchange current (i_o) were calculated. More detailed description of this analysis has been reported elsewhere [16].

2.4. Wet peroxide oxidation experiments

The oxidation tests were carried out batch-wise in a magnetically stirred three-necked glass reactor equipped with a reflux condenser. In a typical experiment, 45 mL of aqueous phenol solution (5 g/L) at pH 3.5 (HCl) were placed in the reactor, along with 0.125 g of activated carbon and the content was heated to 80 °C. Once this temperature was reached, 5 mL of an adjusted concentration of hydrogen peroxide solution were injected and the stirring at 1200 rpm started. Effluents at different reaction times were taken from the reactor and immediately analyzed. After 24 h of reaction, the heating was switched-off and the flask cooled to room temperature in cold water. Then, the catalyst was separated by filtration (0.45 μm Nylon filter) and oven-dried at 60 °C. Additionally, homogenous contribution was assessed by working in the absence of catalyst (blank experiment). Hydrogen peroxide decomposition experiments with activated carbons in the absence of phenol were also carried out. Adsorption runs were performed under the same operating conditions and procedure as the oxidation tests but in the

Table 1
Characterization of the activated carbons.

Sample	d_{002} (Å)	L_c (Å)	L_a (Å)	S_{BET} (m²/g)	A_{ext} (m²/g)	V_m (m³/g)	CO_2 (μmol/g)	CO (μmol/g)
AC-M	3.61	37.99	17.67	1019	175	0.38	30	320
w-AC-M	–	–	–	416	147	0.11	255	483
AC-P	3.79	35.99	16.22	931	472	0.19	131	730
w-AC-P	–	–	–	489	252	0.11	219	674
4th use AC-P	–	–	–	302	264	0.04	1358	2565
Reg. AC-P	–	–	–	920	443	0.22	535	4741

absence of hydrogen peroxide. All the experiments were performed by triplicate being the standard deviation always less than 5%.

2.5. Analytical methods

The organic compounds in the effluent were identified and quantified by high performance liquid chromatography (HPLC, Varian, Mod. ProStar) and ionic chromatography (IC, Metrohm, mod. 883 BASIC IC Plus). Phenol and the aromatic intermediates resulting from oxidation were separated by a Nucleosil C18 5 mm column (Microsob-MV, 15 cm long, 4.6 mm diameter) using a mixture of 4 mM H_2SO_4 aqueous solution at 1 mL/min as mobile phase. A diode array detector at wavelengths of 210 and 246 nm was used. Short-chain organic acids were determined by IC with anionic chemical suppression using a conductivity detector. A Metrosep A supp 5–250 column (25 cm long, 4 mm diameter) was used as stationary phase and 0.7 mL/min of an aqueous solution 3.2 mM of Na_2CO_3 and 1 mM of $NaHCO_3$ as mobile phase. Total organic carbon (TOC) was measured in a Shimadzu TOC V_{SCH} analyzer. Metal content in the liquid effluent was analyzed by TXRF. Hydrogen peroxide concentration was quantified by colorimetric titration using the titanium sulfate method [18]. The presence of hydroxyl radicals was visualized by the methylene blue dye test. Effluents at different reaction times were drop-sampled on a blue methyl tip prepared according to Satoh et al. protocol [19]. The bleaching of the tip corresponds to the oxidation of methylene blue dye (dark blue color) to methyl blue radical cation (colorless) by the hydroxyl radicals.

3. Results and discussion

3.1. Activated carbon characterization

Table 1 collects some structural and textural characteristics of the activated carbons, along with the amounts of CO and CO_2 evolved upon TPD. The elemental analysis results are summarized in Table 2. The corresponding XRD, BET isotherms and TPD profiles are supplied in Figs. S1–S3 of Supporting Information.

Looking at the values of the parameters calculated from the XRD profiles (see Supporting Information, Fig. S1), namely the interlayer spacing value (d_{002}) and the height (L_c) and width (L_a) of the crystalline domains, given in Table 1, both activated carbons are amorphous materials but with different level of disorder. The lower d_{002} and higher L_a and L_c values of AC-M indicate a less-disordered carbon structure than that of AC-P.

Table 2
Elemental analysis of the activated carbons (%, dry bases).

Sample	C	H	N	S	Ashes[a]	O[b]
AC-M	89.3	0.9	0.5	0.6	4	4.7
AC-P	93.7	0.8	0.3	0.1	1	4.1
4th use AC-P	81.0	1.8	0.2	0.06	1	15.9
Reg. AC-P	74.5	2.1	0.2	0.05	1	22.2

[a] Data provided by the supplier.
[b] Calculated by difference.

The textural analyses from N_2 adsorption–desorption isotherms (provided in Supporting Information, Fig. S2) indicates that both carbons have close values of BET surface area but AC-P shows significantly higher contribution of mesoporosity according to the values of the external or non-microporous area (A_{ext}) and the micropore volume (V_m). With regard to chemical composition, the main differences arise from the amount of surface oxygen groups (Table 1) and the ash-content (Table 2), higher in the case of AC-P and AC-M, respectively. Several metallic elements (Ca, Ti, V, Cr, Fe) were identified in the ashes by TXRF, being the content of Fe quite low, 0.04 wt% for AC-M and 0.01 wt% for AC-P. These metallic elements, in particular Fe, must be taken into consideration due to their catalytic effect on hydrogen peroxide decomposition [16]. After phenol prewashing both carbons showed significantly lower BET surface area as a consequence of phenol adsorption, which reduces the available surface for N_2. The micropore volume was significantly reduced after this treatment in the case of w-AC-M but in a much less extent in the case of w-AC-P indicating that the latter maintains the micropores accessible, likely thanks to the most developed external area.

3.2. Hydrogen peroxide decomposition

In a previous work [16], the activity of carbon materials, *viz.* activated carbons (*i.e.* AC-M and AC-P), carbon blacks and graphites for hydrogen peroxide decomposition was evaluated through the values of the apparent first-order rate constant (k_d) and a linear dependence was found between those values and the exchange current (i_o) measured by cyclic voltammetry (see Fig. S4 of Supporting Information). The results demonstrated the supremacy of AC-M over AC-P, exhibiting the former twice the activity of the second because the effect of metallic species (most in particular Fe) prevails over the other physico-chemical features.

Herein, to learn more on the catalytic activity of the activated carbons for hydrogen peroxide decomposition in CWPO, cyclic voltammetry measurements of ACs with phenol adsorbed (w-AC-M and w-AC-P) were now programmed, with the purpose of reproducing the surface conditions in CWPO. The voltammograms are given in Figs. 1 and 2, along with those previously reported for fresh AC-M and AC-P [16] for the sake of comparison. The values of coulombic charge (CC), calculated from the background area of the voltammograms displayed in Fig. 1, and those of the exchange current (i_o), calculated from Fig. 2, are collected in Table 3. Interestingly, the coulombic charge of w-AC-M and w-AC-P decreased

Table 3
Electrochemical properties of the activated carbons and values of the first-order rate constant for hydrogen peroxide decomposition.

Sample	Coulombic charge (mC)	i_o (A/g)	k_d (L/h g)	r^2
AC-M	5.93	0.232	0.420	0.993
w-AC-M	1.42	0.073	0.067	0.992
AC-P	4.60	0.147	0.228	0.983
w-AC-P	1.37	0.045	0.034	0.979
4th use AC-P	1.08	0.017	0.007	0.981
Reg. AC-P	3.37	0.157	0.281	0.991

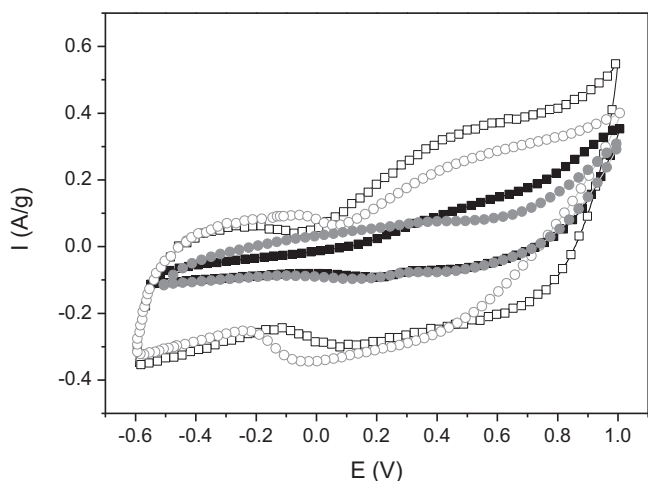**Fig. 1.** Cyclic voltammograms of the fresh and pre-washed activated carbons. Operating conditions: $v = 10$ mV/s, $T = 25\,°C$, pH 3.5 (HCl); (□) AC-M, (■) w-AC-M, (○) AC-P, (●) w-AC-P.

Fig. 2. Cyclic voltammograms of activated carbons in the presence of hydrogen peroxide. Operating conditions: $C_{H_2O_2} = 25$ g/L, $v = 10$ mV/s, $T = 25\,°C$, $pH = 3.5$ (HCl); (□) AC-M, (■) w-AC-M, (○) AC-P, (●) w-AC-P.

around 70% with respect to the fresh carbons (Table 3). This reduction must be associated with the adsorbed phenol located on the electro-deficient sites of the carbon surface [20], thus covering an important part of the active sites. Consequently, only a small amount of them will be now available for hydrogen peroxide decomposition. On the other hand, the values of the exchange current (see i_o values in Table 3) significantly decreased compared to those of the corresponding starting materials. Those results evidence that phenol and hydrogen peroxide compete for the same active sites.

The exchange current value decreases from the fresh carbons to the pre-washed ones but their voltammograms maintain the same shape (Fig. 2) indicating that the redox cycle remains unchanged in the presence of phenol. Kinetic studies of hydrogen peroxide decomposition with the pre-washed carbon samples were carried out for the sake of confirming their cyclic voltammetry behavior. The values of the pseudo-first order rate constant (k_d) are collected in Table 3. The activity ranking derived from these values is in
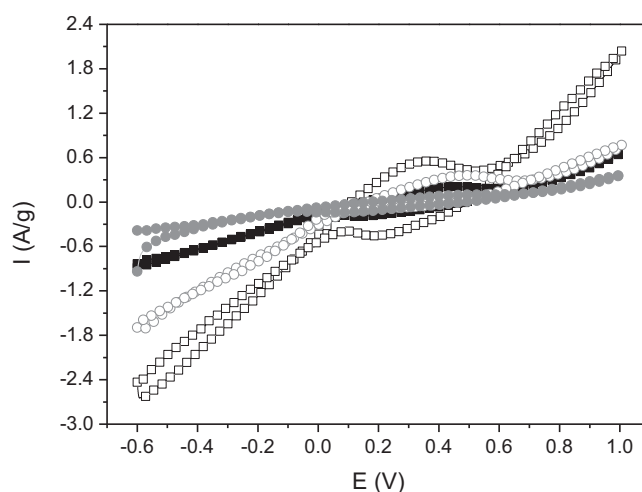
agreement with the predicted from the cyclic voltammetry results: AC-M > AC-P > w-AC-M > w-AC-P. The k_d and i_o values of the phenol pre-washed carbons can be also fitted to the linear correlation obtained for the fresh carbons (Fig. 4S, Supporting Information), which indicates that the activity of the available sites remain unaltered.

In conclusion, the accessibility of hydrogen peroxide to the active sites is hindered by the presence of phenol when relatively high concentrations (5 g/L in this case) are used and, consequently, the rate of hydrogen peroxide decomposition in CWPO will slow down.

3.3. Catalytic wet peroxide oxidation of phenol

The time-evolution of phenol, hydrogen peroxide and TOC conversions under the selected operating conditions (at hydrogen peroxide dose corresponding to the stoichiometric amount for
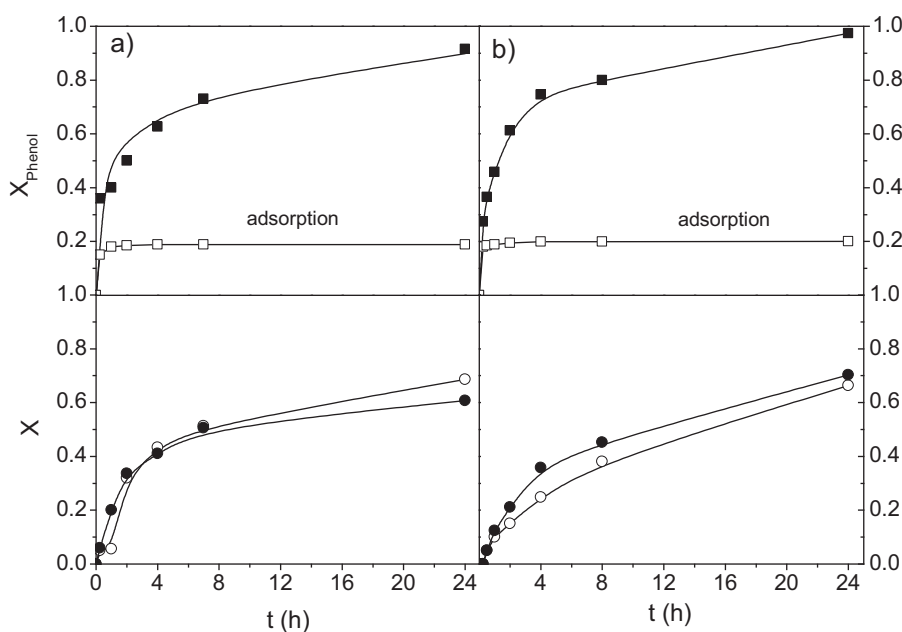

Fig. 3. Time-evolution of phenol (■), H_2O_2 (○) and TOC (●) conversions upon CWPO with AC-M (a) and AC-P (b). Operating conditions: $C_{Phenol,o} = 5$ g/L, $C_{H_2O_2,o} = 25$ g/L, $C_{cat} = 2.5$ g/L, $T = 80\,°C$ and pH_o 3.5.
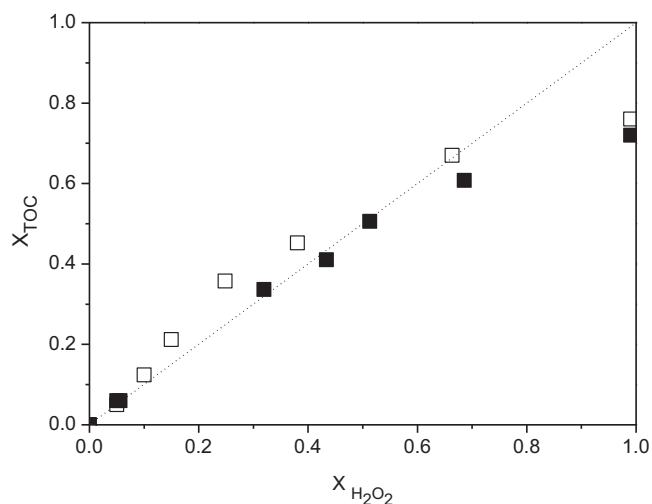
Fig. 4. TOC vs H_2O_2 conversions at the operating conditions of Fig. 3; (■) AC-M, (□) AC-P.

complete mineralization of phenol), are shown in Fig. 3. The concentration of Fe in the liquid effluent after 24 h reaction was 0.25 and 0.02 mg/L for AC-M and AC-P, respectively. Therefore, homogeneous contribution due to Fe in solution can be considered negligible. For the sake of discrimination between adsorption and reaction, the phenol adsorption curves obtained in the absence of hydrogen peroxide are also included. As observed, the adsorption capacity is similar for both carbons, about 20% of phenol being adsorbed under the operating conditions. Also, the adsorption kinetics were similar, since the same time was required to reach the equilibrium concentration with both carbons, around 30 min. Phenol conversions above 95% were achieved after 24 h reaction time, whereas around 20% was achieved in the absence of the activated carbons (Fig. S5 of Supporting Information). As expected, according to the higher content of ashes, AC-M exhibited higher initial activity for hydrogen peroxide decomposition than AC-P and therefore, a faster initial TOC reduction was observed with the former. However, somewhat higher phenol and TOC conversions were achieved with the second at the end of the 24 h-experiments.

TOC vs hydrogen peroxide conversion values are plotted in Fig. 4. As can be seen, 100% efficiency was maintained in the case of AC-M up to hydrogen peroxide conversion around 65% (24 h reaction). Beyond that value, further consumption of hydrogen peroxide was not associated to an equivalent TOC abatement, which remained around 70% even in a three-day experiment in spite of the fact that complete hydrogen peroxide decomposition was achieved. This is

due to the refractoriness of some short-chain organic acids identified as oxidation by-products.

In the case of AC-P, TOC conversions were systematically higher than H_2O_2 conversions up to values of 50% $X_{H_2O_2}$. The only explanation found for these results is that part of the TOC is removed by adsorption of phenol and aromatic intermediates. AC-P, with a more developed mesoporous structure (Table 1), might benefit the reactant surface distribution resulting in a more favored adsorption. This adsorption contribution can also explain the aforementioned somewhat higher phenol conversions obtained with this catalyst compared to those for AC-M.

3.3.1. Oxidation route

The distribution of intermediates and by-products from CWPO of phenol with AC-P is shown in Fig. 5 in terms of equivalent carbon concentration. The same oxidation species and a similar distribution were obtained with AC-M (Fig. S6 of Supporting Information). The intermediates detected were aromatic compounds, such as catechol, resorcinol, hydroquinone and p-benzoquinone, and the by-products were low molecular weight organic acids, such as maleic, malonic, acetic, oxalic and formic. Both groups of reaction products were identified from the earliest stages of the process, which indicates that phenol can be either attacked by hydroxyl radicals in selective meta, orto or para positions, leading to the formation of catechol, resorcinol and hydroquinone, respectively (Fig. 5a), or simultaneously attacked by several hydroxyl radicals in different positions yielding carboxylic acids upon ring opening (Fig. 5b). The aromatic intermediates showed a maximum at around 1 h of reaction time and finally, were completely converted to carboxylic acids whose their residual concentration represented close to 25% of the initial phenol, in terms of carbon.

The TOC values calculated from the identified by-products were fairly close to the experimental TOC measurements (the time-profile evolution is provided in Fig. S7, Supporting Information). The color of the effluents turned from yellowish at short reaction times into colorless after 24 h reaction. Thus the presence of condensation by-products in the liquid effluent, typically detected in Fenton oxidation [21] can be considered negligible.

A remarkable benefit of the use of activated carbons in wet peroxide oxidation is the lower amount of highly ecotoxic by-products in comparison with the homogeneous oxidation process (blank experiment, Fig. S8, Supporting Information). In particular, the concentration of hydroquinone, the most ecotoxic species [22], was 7 times lower in catalytic than in homogeneous oxidation (Fig. S8). The aromatic intermediates were completely converted after 24 h of reaction in the case of CWPO, whereas concentrations up to 325 mg C/L of catechol were still remaining upon the same reaction time of homogeneous oxidation.
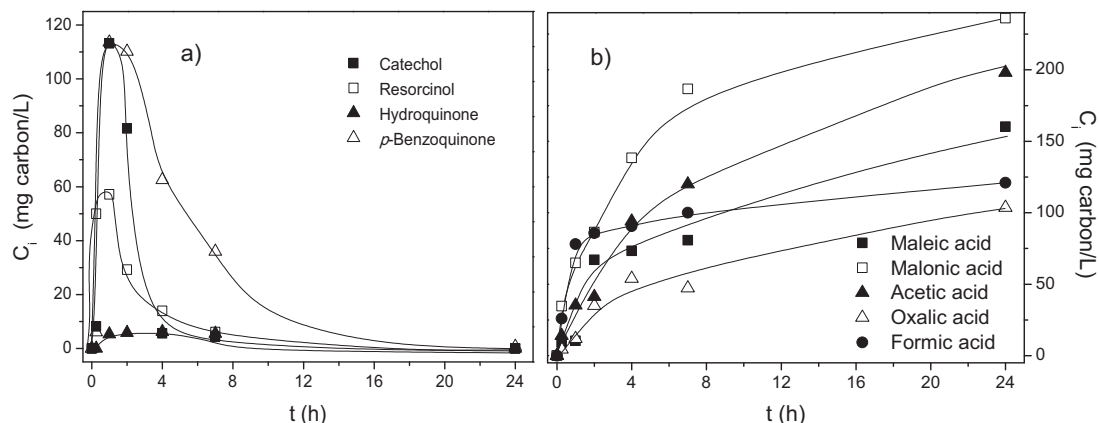

Fig. 5. Time-evolution of intermediates (a) and by-products (b) upon CWPO of phenol with AC-P at the operating conditions of Fig. 3.
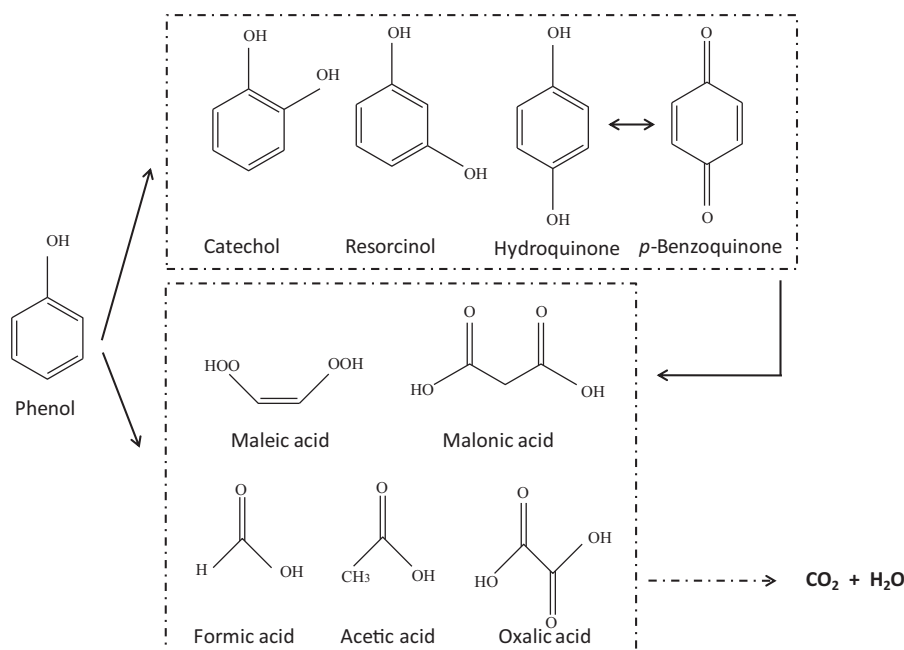
Fig. 6. Reaction pathway of CWPO of phenol with activated carbon.

From the concentration profiles of Fig. 5, the parallel-series reaction pathway of Fig. 6 is proposed. The carboxylic acids could be completely mineralized under appropriate operating conditions [23]. The fact that resorcinol was not detected in homogeneous wet peroxide oxidation, reveals that the oxidation of phenol in the presence of AC takes place simultaneously on the carbon surface, where hydroxyl and hydroperoxy radicals are formed, and in the liquid phase, where the radicals are released (as detected by the methylene blue dye test, Fig. S9, Supporting Information).

3.3.2. Catalyst stability and reusability

Four successive experiments of CWPO were carried out with AC-P. After each run, the carbon was separated by filtration and dried at 60 °C for 24 h without any further treatment. The phenol, TOC and hydrogen peroxide conversion values at 8 and 24 h reaction times in the different cycles (24 h each) are shown in Fig. 7a and b respectively. As can be seen, phenol and TOC abatement gradually decreased upon the successive runs consistently with the progressive decrease of hydrogen peroxide conversion. Noteworthy, the difference between the TOC and hydrogen peroxide conversion values at high reaction times seems to increase with

the cycles (Fig. 7b). Apparently, the efficiency of hydrogen peroxide consumption tends to decrease.

The decreased ability of the activated carbon to decompose hydrogen peroxide was also evidenced by cyclic voltammetry. The initial coulombic charge of 1.37 mC measured for w-AC-P was reduced to 1.08 mC after the 4th use (Table 3). The reason is the reduction of the specific surface area [16] caused by the reaction species adsorbed or deposited on the carbon surface (see S_{BET} values of the w-AC-P and 4th use AC-P in Table 1). Consequently, the carbon active sites for hydrogen peroxide reduction, involved in hydroxyl radical formation, become unavailable upon CWPO. This fact is demonstrated by the 63% decrease in the exchange current (cf. i_o in Table 3, calculated from Fig. 8), which is the most important variable governing carbon activity [16].

The causes of the deactivation can be analyzed on the basis of the results from the characterization of the 4th use AC-P. The BET surface area and micropore volume significantly decreased with respect to the pre-washed carbon (Table 1), whereas the external area remained almost similar. Besides, the elemental analysis of the used carbon presents some significant differences with the fresh one (Table 2). These alterations can be attributed to the presence of
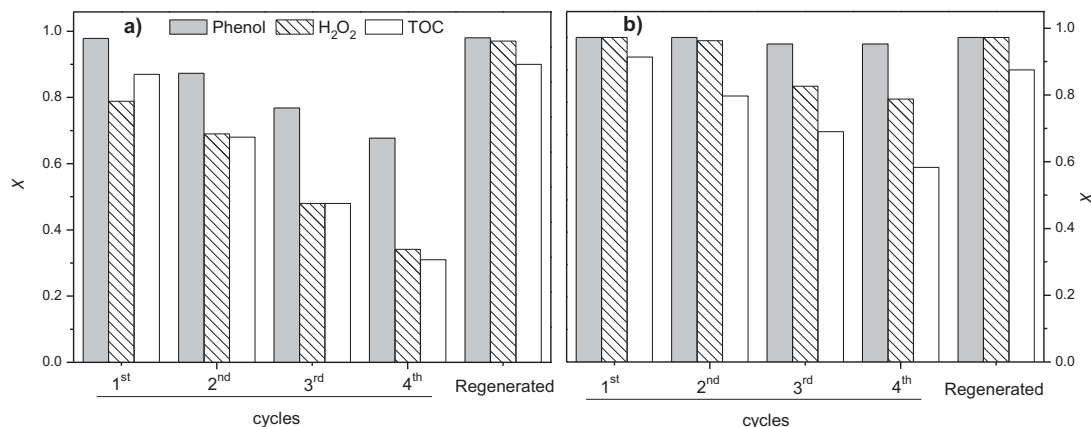

Fig. 7. Performance of AC-P in successive experiments at 8 h (a) and 24 h (b) reaction time: $C_{Phenol,o}$ = 1 g/L, $C_{H_2O_2,o}$ = 5 g/L, C_{cat} = 5 g/L, and pH_o 3.5.

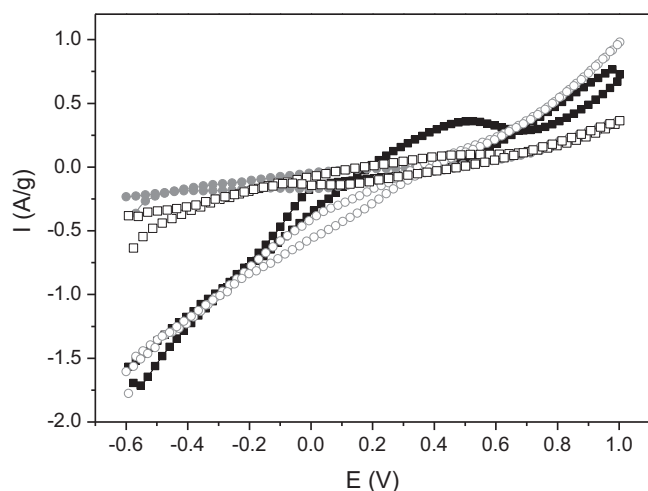**Fig. 8.** Cyclic voltammograms of fresh and used AC-P in the presence of H_2O_2. Operating conditions: $C_{H_2O_2,o} = 25$ g/L, $v = 10$ mV/s, 25 °C, pH 3.5 (HCl); (■) AC-P (□) w-AC-P, (●) 4th use AC-P, (○) Reg. AC-P.

carbonaceous material (*i.e.* phenol, aromatic intermediates, condensation products) adsorbed on the carbon surface that block the access of N_2 to the micropores and would explain the relative decrease of C and the increase of H and O in the elemental analysis. In this sense, the amounts of CO_2 and CO evolved upon TPD up to 1100 °C (Table 1) from AC-P and 4th use AC-P (see Fig. S3 of Supporting Information for TPD profiles) show that CWPO dramatically affects the surface composition, the AC-P catalyst being strongly functionalized upon this treatment. Table 3 summarizes the assessment of the SOGs from the deconvolution of the TPD profiles. As can be observed, the amount of each type of group (carboxylic acid, lactone, anhydride from evolved CO_2 and anhydride, phenol, ether and carbonyl/quinone from CO) has increased, in particular, carboxylic acid, lactone and anhydride. In addition, CO_2 evolved from 600 to 800 °C revealed the presence of new groups such as pyrone.

TGA-DTG analysis of the fresh, pre-washed, and used (2nd and 4th use) AC-P carbon in air atmosphere was carried out and the results are depicted in Fig. 9. The pre-washed and used carbons, specially the 4th use, show higher weight-loss percentage than the fresh one due to the burn-off of adsorbed phenol and oxidation products. The DTG of the phenol-pre-washed carbon shows a smooth band centered around 200 °C which can be assigned to phenol burn-off whereas the 4th

use carbon shows a clearly-seen peak at higher temperatures (350 °C) which can be assigned to the burn-off of condensation species adsorbed on the carbon surface. These are oligomers progressively formed upon the oxidation process since that peak scarcely appears in the 2nd use carbon. The oxidative coupling of phenol on the carbon surface stimulated by the presence of radicals has been already reported in the literature [24,25].

It is of practical interest to learn on the regeneration of the activated carbon. The regeneration of activated carbons affected by phenol-like oligomers has been studied by wet air oxidation at 150–240 °C and 0.2–1 MPa [26] and catalytic air oxidation at 240–300 °C in air [27]. In our case, we have checked a simple oxidative thermal regeneration at temperature somewhat higher than 300 °C according to the DTG but below that of AC burn-off (500 °C). The heating of the 4th use AC-P at 350 °C in air atmosphere (Hobersal, Model 10-PR/200 oven) during 24 h resulted in almost complete removal of the carbon deposits (see DTG of regenerated carbon in Fig. 9) with a fair recovery of the textural properties of the AC (see S_{BET}, A_{ext} and V_m in Table 1). The regeneration process provoked an important decrease of the most acidic SOGs, those decomposing at around 350 °C in the regeneration treatment. As seen in Table 4 (*cf.* 4th use and Reg. AC-P), carboxylic acid groups were depleted, while the amount of lactone and anhydride groups was significantly reduced. In addition, the regeneration in air atmosphere induced the creation of less acidic groups, such as phenol, ether and carbonyl/quinone (Table 4), which might be originated by the oxidation of the most acid groups. Then, the carbon surface does not recover its original chemical composition after the regeneration treatment (*cf.* fresh and Reg. AC-P in Table 4 and elemental analysis in Table 2). Carboxylic acid groups disappear, pyrone groups are now present and the rest of the SOGs are in significant higher amounts. These groups make up the chemical composition of the carbon surface since the carbonaceous deposits were mostly removed (see DTG of regenerated carbon in Fig. 9).

Cyclic voltammetry proved that in spite of the higher amount of SOGs of the regenerated AC-P compared to the fresh one, the electrochemical properties of the starting carbon were recovered (Fig. 8 and Table 3). The exchange current value was even slightly increased (0.156 A/g for Reg. AC-P *vs.* 0.147 for as-received AC-P), and consequently, the apparent kinetic constant for hydrogen peroxide decomposition was higher for the regenerated than for the fresh AC-P (Table 3). These results demonstrate that the accessibility of the carbon active sites has been restored as well as the catalyst performance (Fig. 7).
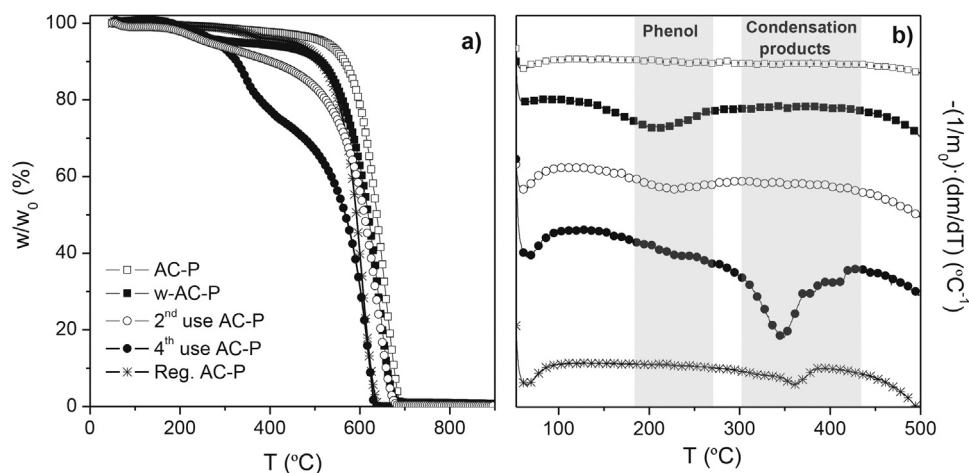

Fig. 9. TGA (a) and DTA (b) of fresh, spent and Reg. AC-P in air at 10 °C/min heating rate.

Table 4
Assessment of surface oxygen groups from deconvolution of TPD profiles for AC-P.

Sample	Groups evolved as CO_2 (μmol/g)				Groups evolved as CO (μmol/g)			
	Carboxylic	Anhydride	Lactone	Pyrone	Anhydride	Phenol	Ether	Carbonyl[a]
AC-P	59	50	22	0	34	119	278	299
4th use AC-P	646	469	154	88	315	967	897	385
Reg. AC-P	0	105	345	85	0	1673	2454	613

[a] Included carbonyl, quinone, chromene.

4. Conclusions

Activated carbons can act as efficient catalysts in the wet peroxide oxidation of phenolic wastewater if the operating conditions are adequate. Working under pollutant concentration and pollutant/carbon mass ratios higher than those commonly used in the literature so far allows avoiding or significantly reducing the non-effective consumption of hydrogen peroxide in parasitic reactions thus giving rise to improved efficiency (*i.e.* 97% phenol and 70% TOC conversions were achieved at 80 °C and 24 h with AC-P).

Under these operating conditions, great part of the carbon surface is occupied by phenol and the amount of active sites available is reduced. As a consequence, more controllable hydrogen peroxide decomposition into hydroxyl and hydroperoxy radicals takes place and these species efficiently react with phenol in the vicinity of the carbon surface, reducing parasitic recombination and allowing a more efficient consumption of hydrogen peroxide.

Phenol is oxidized in a parallel-series reaction pathway where all the intermediate products, aromatics such as catechol, resorcinol hydroquinone and *p*-benzoquinone, and by-products low molecular weight acids, such as maleic, malonic, acetic, oxalic and formic were successfully identified. Condensation by-products remained adsorbed on the carbon surface which represents an important advantage regarding to wastewater cleaning but provokes the progressive deactivation of these AC catalyst. Nevertheless, the activity can be recovered by simple oxidative thermal regeneration at 350 °C.

Acknowledgment

Appendix A. Supplementary data

Supplementary data associated with this article can be found, in the online version, at http://dx.doi.org/10.1016/j.apcatb.2013.04.068.

References

[1] A. Dhaouadi, N. Adhoum, Applied Catalysis B: Environmental 97 (2010) 227–235.
[2] J.A. Zazo, J.A. Casas, A.F. Mohedano, J.J. Rodriguez, Applied Catalysis B: Environmental 65 (2006) 261–268.
[3] F. Duarte, F.J. Maldonado-Hodar, L.M. Madeira, Applied Catalysis B: Environmental 103 (2011) 109–115.
[4] L.C.A. Oliveira, C.N. Silva, M.I. Yoshida, R.M. Lago, Carbon 42 (2004) 2279–2284.
[5] V.P. Santos, M.F.R. Pereira, P.C.C. Faria, J.J.M. Orfao, Journal of Hazardous Materials 162 (2009) 736–742.
[6] O. Taran, E. Polyanskaya, O. Ogorodnikova, V. Kuznetsov, V. Parmon, M. Besson, C. Descorme, Applied Catalysis A-General 387 (2010) 55–66.
[7] H.T. Gomes, S.M. Miranda, M.J. Sampaio, A.M.T. Silva, J.L. Faria, Catalysis Today 151 (2010) 153–158.
[8] F. Lücking, H. Köser, M. Jank, A. Ritter, Water Research 32 (1998) 2607–2614.
[9] H.H. Huang, M.C. Lu, J.N. Chen, C.T. Lee, Chemosphere 51 (2003) 935–943.
[10] A. Georgi, F.D. Kopinke, Applied Catalysis B: Environmental 58 (2005) 9–18.
[11] A. Rey, M. Faraldos, A. Bahamonde, J.A. Casas, J.A. Zazo, J.J. Rodriguez, Industrial & Engineering Chemistry Research 47 (2008) 8166–8174.
[12] L.F. Liotta, M. Gruttadauria, G. Di Carlo, G. Perrini, V. Librando, Journal of Hazardous Materials 162 (2009) 588–606.
[13] S. Navalon, A. Dhakshinamoorthy, M. Alvaro, H. Garcia, ChemSusChem 4 (2011) 1712–1730.
[14] M. Kimura, I. Miyamoto, Bulletin of the Chemical Society of Japan 67 (1994) 2357–2360.
[15] A. Rey, J.A. Zazo, J.A. Casas, A. Bahamonde, J.J. Rodriguez, Applied Catalysis A-General 402 (2011) 146–155.
[16] C.M. Domínguez, A. Quintanilla, P. Ocón, J.A. Casas, J.J. Rodriguez, The use of cyclic voltammetry to assess the activity of carbon materials for hydrogen peroxide decomposition, Carbon (2013), http://dx.doi.org/10.1016/j.carbon.2013.03.058.
[17] L.B. Khalil, B.S. Girgis, T.A.M. Tawfik, Journal of Chemical Technology and Biotechnology 76 (2001) 1132–1140.
[18] G.M. Eisenberg, Industrial and Engineering Chemistry-Analytical Edition 15 (1943) 327–328.
[19] A.Y. Satoh, J.E. Trosko, S.J. Masten, Environmental Science and Technology 41 (2007) 2881–2887.
[20] J.M.V. Nabais, J.A. Gomes, Suhas, P.J.M. Carrott, C. Laginhas, S. Roman, Journal of Hazardous Materials 167 (2009) 904–910.
[21] J.A. Zazo, J.A. Casas, A.F. Mohedano, M.A. Gilarranz, J.J. Rodriguez, Environmental Science and Technology 39 (2005) 9295–9302.
[22] A. Santos, P. Yustos, A. Quintanilla, F. Garcia-Ochoa, J.A. Casas, J.J. Rodriguez, Environmental Science and Technology 38 (2004) 133–138.
[23] H. Debellefontaine, M. Chakchouk, J.N. Foussard, D. Tissot, P. Striolo, Environmental Pollution 92 (1996) 155–164.
[24] T.M. Grant, C.J. King, Industrial and Engineering Chemistry Research 29 (1990) 264–271.
[25] E.Y. OseiTwum, N.S. Abuzaid, G. Nahkla, Bulletin of Environmental Contamination and Toxicology 56 (1996) 513–519.
[26] V.D. Mundale, H.S. Joglekar, A. Kalam, J.B. Joshi, Canadian Journal of Chemical Engineering 69 (1991) 1149–1159.
[27] Y.I. Matatov-Meytal, M. Sheintuch, G.E. Shter, G.S. Grader, Carbon 35 (1997) 1527–1531.